Med Oncol (2016)33:130
DOI 10.1007/s12032-016-0840-y

ORIGINAL PAPER

Identification of candidate biomarkers and analysis of prognostic values in ovarian cancer by integrated bioinformatics analysis

Zhanzhan Xu[1] · Yu Zhou[1] · Yexuan Cao[2] · Thi Lan Anh Dinh[2] · Jing Wan[2] · Min Zhao[1]

Received: 6 September 2016 / Accepted: 5 October 2016

Abstract Ovarian cancer is the first leading cause of mortality in gynecological malignancies. To identify key genes and microRNAs in ovarian cancer, mRNA microarray dataset GSE36668, GSE18520, GSE14407 and microRNA dataset GSE47841 were downloaded from the Gene Expression Omnibus database. Differentially expressed genes (DEGs) and microRNAs (DEMs) were obtained using GEO2R. Functional and pathway enrichment analysis were performed for DEGs using DAVID database. Protein–protein interaction (PPI) network was established by STRING and visualized by Cytoscape. Following, overall survival (OS) analysis of hub genes was performed by the Kaplan–Meier plotter online tool. Module analysis of the PPI network was performed using MCODE. Moreover, miRecords was applied to predict the targets of the DEMs. A total of 345 DEGs were obtained, which were mainly enriched in the terms related to cell cycle, mitosis, and ovulation cycle process. A PPI network was constructed, consisting of 141 nodes and 296 edges. Sixteen genes had high degrees in the network. High expression of four genes of the 16 genes was associated with worse OS of patients with ovarian cancer, including *CCNB1*, *CENPF*, *KIF11*, and *ZWINT*. A significant module was detected from the PPI network. The enriched functions and pathways included cell cycle, nuclear division, and oocyte meiosis. Additionally, a total of 36 DEMs were identified. The expression of *KIF11* was negatively correlated with that of has-miR-424 and has-miR-381, and it was also the potential target of two microRNAs. In conclusion, these results identified key genes, which could provide potential targets for ovarian cancer diagnosis and treatment.

Keywords Ovarian caner · Differentially expressed genes · Functional enrichment analysis · Protein–protein interaction · Kaplan–Meier plotter

Introduction

Ovarian cancer is the most lethal gynecological malignancy worldwide, with an estimated 238,700 new cases of ovarian cancer and estimated 151,190 deaths from this disease every year [1]. The high mortality of ovarian cancer is mainly due to the lack of effective diagnostic methods at early stage and high recurrence rate [2]. With the vagueness of symptoms, approximately 70 % of patients are diagnosed with ovarian cancer at an advanced stage, in which the 5-year survival rate is less than 25 % compared to up to 90 % for patients diagnosed with this tumor in early prophase [3, 4].

Currently, molecular biomarkers have been developed for diagnostic use in ovarian cancer. For example, carbohydrate antigen-125 (CA-125) is the most extensively applied serum biomarker for ovarian cancer [5]. But CA-125 is highly expressed in common benign and malignant conditions, and only elevated by about 50 % of early stage ovarian cancers [6, 7]. Human epididymis protein 4 (HE4) is another biomarker for ovarian cancer that has a greater specificity and a less sensitivity than CA-125 [8]. Nevertheless, to date, no detecting technology is suited to

✉ Min Zhao
minzhao@whu.edu.cn

[1] Department of Biomedical Engineering, School of Basic Medical Sciences, Wuhan University, 185 Donghu Road, Wuhan 430071, Hubei, People's Republic of China

[2] Department of Cardiology, Zhongnan Hospital of Wuhan University, Wuhan 430071, Hubei, People's Republic of China

Published online: 18 October 2016

generable people due to the deficiency of specificity and sensitivity. Accordingly, it is crucial to investigate the molecular mechanisms in ovarian cancer progression and discover additional biomarkers for early effective diagnosis.

In recent years, the microarray technology has been broadly used to obtain general genetic alteration during tumorigenesis [9–12]. The bioinformatics methods are necessary to process a great deal of data generated by microarray technology. In this work, given the false positive in results of microarray, three mRNA microarray dataset and a microRNA dataset were analyzed to obtain differentially expressed genes (DEGs) and microRNAs (DEMs) between ovarian cancer tissues and normal tissues samples. Functional enrichment and network analysis were applied for identifying of DEGs, combined with survival analysis and mRNA–microRNA interaction analysis, to identify key genes in ovarian cancer.

Materials and methods

Microarray data

The Gene Expression Omnibus (GEO, http://www.ncbi.nlm.nih.gov/geo) is a public repository for data storage, such as microarray and next-generation sequencing, which is freely available to users. Three gene expression profiles (GSE36668, GSE18520 and GSE14407) and the miRNA expression profile of GSE47841 were obtained from GEO database. The array data of GSE36668 included four ovarian cancer tissue samples and four normal samples [10]. GSE18520 consisted of 53 ovarian cancer samples and ten normal samples [11]. GSE14407 included 12 ovarian cancer samples and 12 normal samples [9]. The miRNA expression profile of GSE47841 included 12 ovarian cancer samples and nine normal samples [12].

Data processing

The GEO database archives a large number of high-throughput functional genomic studies that contain data that are processed and normalized using various methods. GEO2R (http://www.ncbi.nlm.nih.gov/geo/geo2r/) was applied to screen differentially expressed miRNAs and genes between ovarian cancer and normal samples. GEO2R is an interactive web tool that compares two groups of samples under the same experimental conditions and can analyze almost any GEO series [13]. The adjusted P values (adj. P) were applied to correct for the occurrence of false positive results using Benjamini and Hochberg false discovery rate method by default. The adj. $P < 0.01$ and $|\log FC| > 1$ were set as the cut-off criterion.

Functional and pathway enrichment analysis

The Database for Annotation, Visualization and Integrated Discovery (DAVID, http://david.abcc.ncifcrf.gov/) is an online program that provides a comprehensive set of functional annotation tools for researchers to understand biological meaning behind plenty of genes [14]. Gene ontology (GO) and Kyoto Encyclopedia of Genes and Genomes (KEGG) pathway enrichment analysis were performed for identified DEGs using DAVID database. $P < 0.05$ was set as the cut-off criterion.

PPI network construction and modules selection

The functional interactions between proteins can provide context in molecular mechanism of cellular processing. In present study, protein–protein interaction (PPI) network of DEGs was constructed using the Search Tool for the Retrieval of Interacting Genes (STRING, http://string.embl.de/) database and subsequently was visualized using Cytoscape [15, 16]. And confidence score ≥ 0.7 was set as the cut-off criterion. Then, the Molecular Complex Detection (MCODE) was performed to screen modules of PPI network with degree cutoff = 2, node score cut-off = 0.2, k-core = 2, and max. depth = 100 [17]. The functional enrichment analysis of genes in each module was performed by DAVID.

Prediction of miRNA targets

The target genes of differentially expressed miRNAs were predicted using miRecords (http://c1.accurascience.com/miRecords/), which is an integrated resource produced by 11 established miRNA target prediction programs (DIANA-microT, MicroInspector, miRanda, MirTarget2,

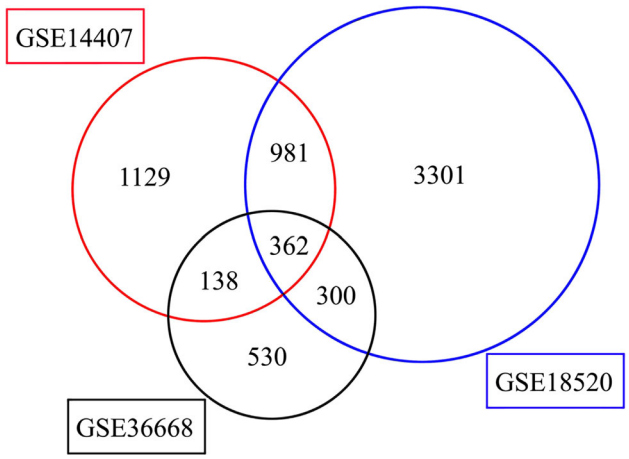

Fig. 1 Identification of differentially expressed genes in mRNA expression profiling datasets GSE36668, GSE18520, and GSE14407

Table 1 Functional and pathway enrichment analysis of up-regulated and down-regulated genes in ovarian cancer

Term	Description	Count	*P* value
Up-regulated			
GO:0022403	Cell cycle phase	33	1.64E−20
GO:0000279	M phase	30	3.58E−20
GO:0000278	Mitotic cell cycle	31	8.00E−20
GO:0022402	Cell cycle process	35	2.24E−18
GO:0007067	Mitosis	24	9.38E−18
GO:0000280	Nuclear division	24	9.38E−18
GO:0000087	M phase of mitotic cell cycle	24	1.40E−17
GO:0048285	Organelle fission	24	2.30E−17
GO:0007049	Cell cycle	38	1.09E−16
GO:0051301	Cell division	24	6.49E−15
KEGG:hsa04110	Cell cycle	10	4.37E−06
KEGG:hsa04114	Oocyte meiosis	7	8.97E−04
KEGG:hsa04115	p53 signaling pathway	5	0.005235
KEGG:hsa05200	Pathways in cancer	10	0.006138
KEGG:hsa05222	Small cell lung cancer	5	0.010976
KEGG:hsa04512	ECM-receptor interaction	5	0.010976
KEGG:hsa00051	Fructose and mannose metabolism	3	0.048362
Down-regulated			
GO:0007548	Sex differentiation	8	3.71E−04
GO:0022602	Ovulation cycle process	5	0.002143
GO:0008585	Female gonad development	5	0.002408
GO:0042698	Ovulation cycle	5	0.002847
GO:0046660	Female sex differentiation	5	0.003169
GO:0046545	Development of primary female sexual characteristics	5	0.003169
GO:0030041	Actin filament polymerization	3	0.004007
GO:0048608	Reproductive structure development	6	0.005078
GO:0009725	Response to hormone stimulus	10	0.005084
GO:0045137	Development of primary sexual characteristics	6	0.005249

If there were more than five terms enriched in this category, top five terms were selected according to *P* value. Count: the number of enriched genes in each term

GO gene ontology, *KEGG* Kyoto Encyclopedia of Genes and Genomes

miTarget, NBmiRTar, PicTar, PITA, RNA22, RNAhybrid, and TargetScan) [18]. The genes predicted by at least four programs were identified as the targets of miRNAs.

Survival analysis of DEGs

Kaplan–Meier plotter (KM plotter, www.kmplot.com) was capable to assess the effect of 54,675 genes on survival using 10,188 cancer samples, including 4142 breast, 1648 ovarian, 2437 lung, and 1065 gastric cancer patients [19]. The patients with ovarian cancer were split into two groups according to the expression of a particular gene (high vs. low expression). The overall survival of patients with ovarian cancer was analyzed using a Kaplan–Meier plot. The hazard ratio (HR) with 95 % confidence intervals and log rank *P* value were calculated and displayed on the webpage.

Results

Identification of DEGs

A total of 1330, 4944 and 2610 DEGs were identified from GSE36668, GSE18520, and GSE14407 datasets, respectively. Three hundred and sixty-two genes were screened out in all three datasets (Fig. 1). Among them, 345 genes presented identical expression trends in all three datasets, consisting of 168 up-regulated genes and 177 down-regulated genes in ovarian cancer tissues compared to normal ovary tissues.

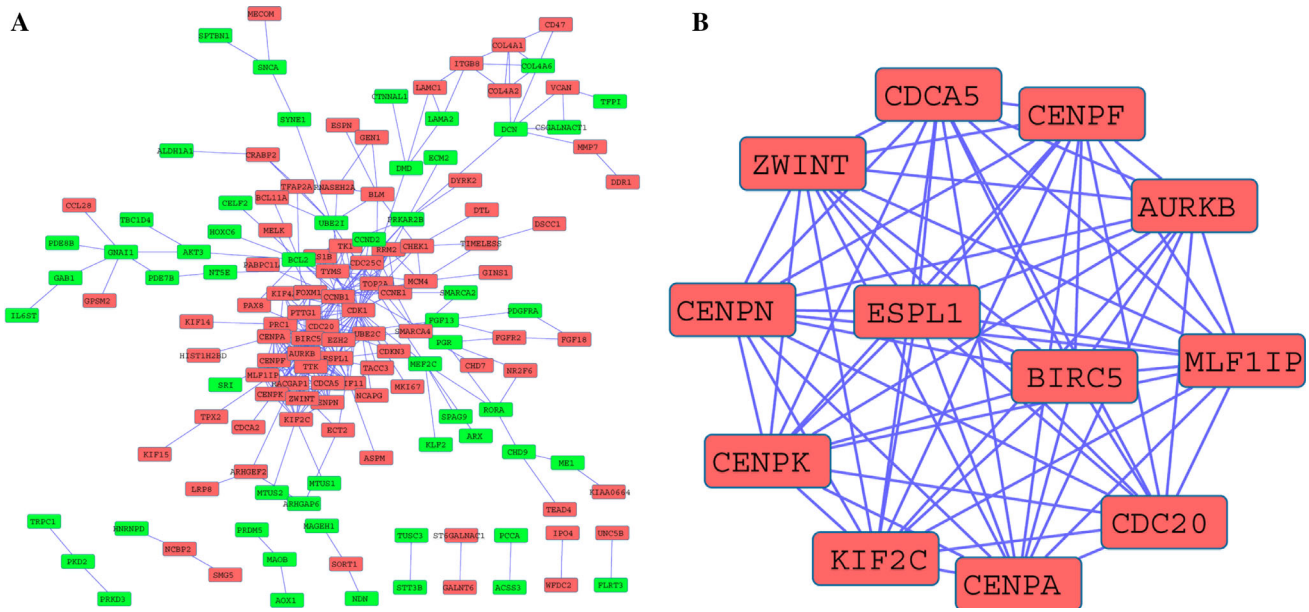

Fig. 2 Protein–protein interaction network and a significant module. **a** Protein–protein interaction network of differentially expressed genes. **b** A significant module selected from protein–protein interaction network. *Red nodes* stand for up-regulated genes, while *green nodes* stand for down-regulated genes. The *lines* represent interaction relationship between nodes

Table 2 Functional and pathway enrichment analysis of the genes in module

Term	Description	Count	*P* value
GO:0000278	Mitotic cell cycle	9	1.25E−11
GO:0000280	Nuclear division	8	3.15E−11
GO:0007067	Mitosis	8	3.15E−11
GO:0000087	M phase of mitotic cell cycle	8	3.58E−11
GO:0048285	Organelle fission	8	4.18E−11
GO:0022402	Cell cycle process	9	3.69E−10
GO:0000279	M phase	8	5.32E−10
GO:0022403	Cell cycle phase	8	2.65E−09
GO:0007049	Cell cycle	9	4.60E−09
GO:0051301	Cell division	7	1.99E−08
KEGG:hsa04114	Oocyte meiosis	2	0.042801
KEGG:hsa04110	Cell cycle	2	0.048565

If there were more than five terms enriched in this category, top five terms were selected according to *P* value. Count: the number of enriched genes in each term

GO gene ontology, *KEGG* Kyoto Encyclopedia of Genes and Genomes

Functional and pathway enrichment analysis

To gain further insight into the function of identified DEGs, functional and pathway enrichment analysis was performed using DAVID. The up-regulated genes were mainly involved in biological processes associated cell cycle and mitosis, while down-regulated genes were mainly enriched in sex differentiation, ovulation cycle process, response to hormone stimulus and reproductive structure development (Table 1). Moreover, seven KEGG pathways were over-represented in up-regulated genes, including cell cycle, oocyte meiosis, and p53 signaling pathway (Table 1). No KEGG pathway was significant for down-regulated genes.

PPI network construction and modules selection

The PPI network of DEGs consisted of 141 nodes and 296 edges, including 86 up-regulated genes and 55 down-

Table 3 Differentially expressed microRNAs in ovarian cancer and their targets

miRNA	Adj. *P*	logFC	Target genes
hsa-mir-200a	3.27E−09	1.821797	*CHD9*, *GINS1*, *CCNE1*, *SPAG9*, *ITGB8*, *CHD7*, *GNAI1*, *PRC1*, *TFAP2A*, *TFPI*
hsa-mir-182	1.19E−06	1.060197	*CD47*, *MEF2C*, *SRI*, *MLF1IP*, *GINS1*, *ITGB8*, *PDE7B*, *PRC1*, *SYNE1*, *COL4A1*
hsa-mir-141	2.67E−06	1.350156	*CD47*, *AOX1*, *MTUS1*, *PRKAR2B*, *GPSM2*, *CHD9*, *CCNE1*, *SPAG9*, *NT5E*, *ITGB8*
hsa-mir-200c	3.18E−06	1.273887	*CD47*, *AKT3*, *PKD2*, *MLF1IP*, *CHD9*, *SORT1*, *SPTBN1*, *ITGB8*, *PDE7B*, *HNRNPD*
hsa-mir-183	4.26E−06	1.439625	*CD47*, *MEF2C*, *PKD2*, *GINS1*, *SPTBN1*, *ITGB8*, *HNRNPD*, *LRP8*, *FLRT3*, *FGF13*
hsa-mir-424	2.10E−08	−1.8945	*CD47*, *KIF11*, *CENPA*, *PAX8*, *ESPN*, *GINS1*, *BIRC5*, *CCNE1*, *SORT1*, *BCL11A*
hsa-mir-381	3.72E−07	−1.3934	*CD47*, *KIF11*, *GINS1*, *AURKB*, *ITGB8*, *PTTG1*, *COL4A1*, *CDC25C*, *FGFR2*, *LAMC1*
hsa-mir-383	8.90E−07	−1.67653	*CD47*, *FOXM1*, *ITGB8*, *CDCA5*, *TFAP2A*, *LAMC1*, *TOP2A*, *DTL*, *BCL11A*
hsa-mir-4324	2.66E−06	−1.35248	NA
hsa-mir-542-5p	4.26E−06	−1.3239	*CD47*, *CRABP2*, *PRC1*, *SORT1*, *DTL*, *ESPN*

A positive logFC value represents that the microRNA is up-regulated in ovarian cancer, while a negative logFC value represents the microRNA is down-regulated in ovarian cancer. If there were more than ten genes predicted by miRecords, only ten genes were listed in table

FC fold change, *NA* not available

regulated genes (Fig. 2a). Degrees ≥10 was set as the cut-off criterion. A total of 16 genes were selected as hub genes, such as *CDK1*, *AURKB*, *CCNB1*, and *CDC20*. Moreover, it was found that cyclin B1 (CCNB1) had interactions with kinesin family member 11 (KIF11) and centromere protein F (CENPF).

A significant module was obtained from PPI network of DEGs using MCODE, including 12 nodes and 66 edges (Fig. 2b). Functional and KEGG pathway enrichment analysis revealed that genes in this module were mainly associated with cell cycle, mitosis and oocyte mitosis (Table 2).

miRNA–DEG pairs

A total of 36 differentially expressed miRNAs were screened out from GSE47841 datasets, consisting of 15 up-regulated and 21 down-regulated miRNAs in ovarian cancer compared with normal ovary sample (control). As shown in Table 3, miR-200a was the most significantly up-regulated miRNA, while miR-424 was the most significantly down-regulated miRNA. Following, based on miRecords database, the predicted targets of miRNAs were obtained. By comparing the targets with DEGs, we found that CD47 was the potential target of eight miRNAs, including has-miR-182, has-miR-141, has-miR-200c, has-miR-183, has-miR-424, has-miR-381, has-miR-383, and has-miR-542-5p. Moreover, KIF11 was potentially targeted by has-miR-424 and has-miR-381, which was consistent with their expression trend in ovarian cancer.

The Kaplan–Meier plotter

The prognostic value of 16 hub genes in PPI network was assessed in www.kmplot.com. Overall survival for patients with ovarian cancer was obtained according to the low and high expression of each gene. It was found that high mRNA expression of *CCNB1* (HR 1.26 [1.01–1.58], $P = 0.04$) was associated with worse overall survival for ovarian cancer patients, as well as *CENPF* (HR 1.18 [1.03–1.35], $P = 0.014$), *KIF11* (HR 1.15 [1–1.31], $P = 0.04$), *ZWINT* (HR 1.15 [1–1.31], $P = 0.04$) (Fig. 3).

Discussion

Despite advances in surgical and medical therapy, the overall mortality of ovarian cancer has remained largely unchanged over the past decades. The lethality of ovarian cancer is mainly due to the difficulties in detecting it at an early stage and lack of effective treatments for patients with an advanced status [20]. Therefore, understanding of the etiological factors and mechanisms of ovarian cancer progression are essential to improve survival rate and prevention. Recently, microarray technology has been developing rapidly and has been widely used to reveal the general genetic alteration in progression of diseases, which enables the identification of targets for diagnosis, therapeutic, and prognosis of tumors.

In this study, a total of 345 DEGs were screened, consisting of 168 up-regulated genes and 177 down-regulated genes. These up-regulated genes were mainly enriched in cell cycle, mitosis and P53 signaling pathway, which were closely related to cancer, while the down-regulated genes were mainly enriched in ovulation cycle and sex differentiation. Among these DEGs, 16 genes had high degrees in the PPI network. Following, survival analysis of these genes revealed that four up-regulated genes were significantly correlated with worse overall survival of patients

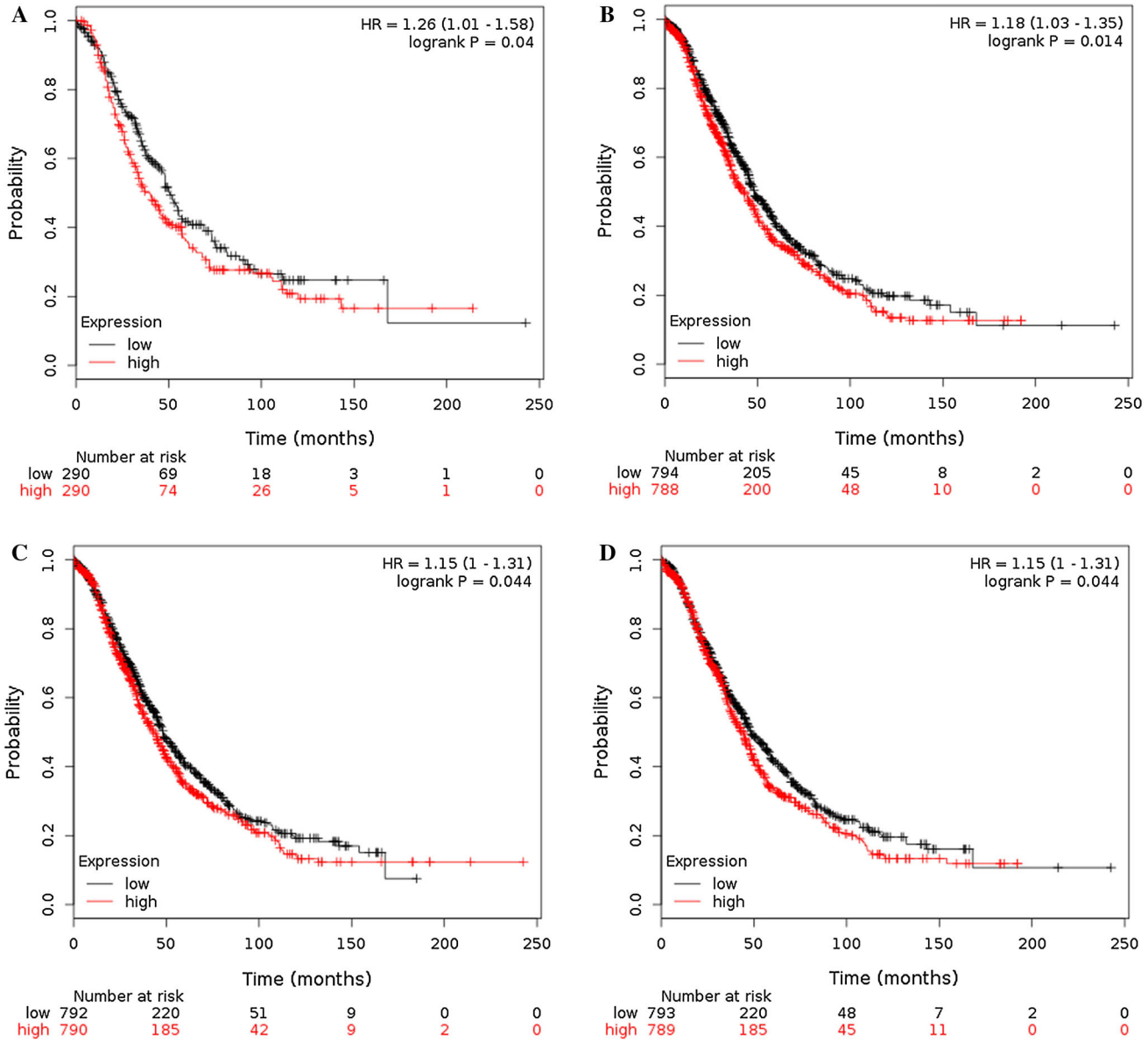

Fig. 3 Prognostic value of four genes in ovarian cancer patients. Prognostic value of *CCNB1* (**a**), *CENPF* (**b**), *KIF11* (**c**) and *ZWINT* (**d**) were obtained in www.kmplot.com. The desired Affymetrix IDs are valid: 228729_at (*CCNB1*), 209172_s_at (*CENPF*), 204444_at (*KIF11*), 204026_s_at (*ZWINT*). *HR* hazard ratio, *CI* confidence interval

with ovarian cancer, including *CCNB1*, *CENPF*, *KIF11,* and *ZWINT*.

The pathogenesis of tumor is a complex process driven by specific genetic and epigenetic alterations. Increased expression of *CCNB1* was found in many different diseases, including colorectal cancer, pancreatic cancer, and melanoma [21–23]. CCNB1 could activate cyclin-dependent kinase (CDK1), which controlled key early mitotic events by initiating the phosphorylation of various proteins at the G2/M transition [24]. The low expression of *CCNB1* could suppress proliferation and induce apoptotic in ovarian cancer [25, 26]. *CENPF*, at chromosome 1q41, encodes a protein that associates with the centromere-kinetochore complex. It was reported that CENPF had two microtubule-binding domains, so it played a role in microtubule attachment and microtubule dynamics during mitosis [27]. Accumulating evidence showed that over-expression of *CENPF* was involved in multiple cancer types such as breast cancer, hepatocellular carcinoma [28, 29]. And Yang et al. found the increased expression of *CENPF* was correlated with poor prognosis in patients with prostate cancer [30]. However, the oncogenic role and clinical significance of *CENPF* for ovarian cancer were rarely explored. In the present study, we found *CCNB1* and *CENPF* were over-

expressed and had interaction, indicating the joint function in ovarian cancer.

As a member of kinesin-like protein family, KIF11 is a critical spindle motor protein during the establishment of a bipolar mitotic spindle. It was reported that inhibition of KIF11 with small-molecule inhibitor could block cell cycle progression, cause abnormal chromosome segregation, and finally lead to cell death in head and neck squamous cell carcinoma [31]. Similar results also showed that KIF11 inhibition suppressed proliferation and invasion in glioblastoma, indicating its potential as an anticancer target [32]. Meanwhile, mutations in *KIF11* were a common cause of a variety of congenital diseases such as microcephaly syndrome and chorioretinal dysplasia [33]. Kinetochore assembly is a key step in cell cycle progression. ZWINT, as a part of kinetochore complex, is a protein interacting with ZW10 that is essential to the chromosome motility and mitotic spindle checkpoint [34]. Endo et al. found that the growth of cells was prompted by stable expression of *ZWINT*, while it was suppressed by targeting *ZWINT* with siRNA in MCF7 breast cancer cells [35]. Taken together, this data suggests that *CCNB1*, *CENPF*, *KIF11,* and *ZWINT* involve in the pathogenesis of malignant tumors by affecting mitosis, and cell cycle process, which support our findings.

A miRNA is a small noncoding RNA molecule that regulates gene expression by targeting 3′ UTR of mRNAs to cause translational repression or degradation [36]. Increasing evidence suggested that dysregulation of miRNAs was responsible for the pathogenesis of multiple cancer types, including ovarian cancer. In the present study, we identified 36 DEMs, consisting of 15 up-regulated and 21 down-regulated miRNAs in ovarian cancer. miR-200a was the most significantly up-regulated miRNA, while miR-424 was the most significantly down-regulated miRNA. Similar results were previously reported that miR-200a and miR-200c showed a significantly higher level in ovarian cancer tissues than healthy tissues and were identified as candidate biomarkers in epithelial ovarian cancer [37, 38]. Xu et al. found that miR-424 could reverse chemoresistance of ovarian cancer cells, and high levels of miR-424 were positively correlated with the progression-free survival of patients with ovarian cancer [39]. Besides, miR-381 also played an important role in the development of ovarian cancer. Overexpression of miR-381 suppressed proliferation, migration, and invasion of ovarian cancer cells [40]. Notably, we found that *KIF11* was potentially targeted by has-miR-424 and has-miR-381, indicating that miR-424 and miR-381 may play a role in ovarian cancer by mediating *KIF11*.

In summary, the current study was intended to identify DEGs with comprehensive bioinformatics analysis to find the potential biomarkers and predict progression of diseases. In our study, a total of 345 DEGs and 36 DEMs were screened out, and *CCNB1*, *CENPF*, *KIF11*, *ZWINT* and several miRNAs such as miR-200a and miR-424 might be key genes related to ovarian cancer. Our results suggested that data mining and integration could be a useful tool to predict progression of ovarian cancer, to understand the mechanism of the occurrence and development of tumor. To apply these gene expression profiles in clinical practice, it is necessary to improve the reliability and reproducibility of analysis model in independent datasets in the future. Nevertheless, our study could provide new cutes for diagnosis and treatment of ovarian cancer patients.

Compliance with ethical standards

Conflict of interest The authors declare that they have no conflicts of interest.

Ethical approval This article does not contain any studies with human participants or animals performed by any of the authors.

References

1. Torre LA, Bray F, Siegel RL, Ferlay J, Lortet-Tieulent J, Jemal A. Global cancer statistics, 2012. CA Cancer J Clin. 2015;65(2):87–108. doi:10.3322/caac.21262.
2. Wright JD, Shah M, Mathew L, Burke WM, Culhane J, Goldman N, et al. Fertility preservation in young women with epithelial ovarian cancer. Cancer. 2009;115(18):4118–26. doi:10.1002/cncr.24461.
3. Urban N, Drescher C. Potential and limitations in early diagnosis of ovarian cancer. Adv Exp Med Biol. 2008;622:3–14. doi:10.1007/978-0-387-68969-2_1.
4. Goff BA, Mandel L, Muntz HG, Melancon CH. Ovarian carcinoma diagnosis. Cancer. 2000;89(10):2068–75.
5. Urban N, Hawley S, Janes H, Karlan BY, Berg CD, Drescher CW, et al. Identifying post-menopausal women at elevated risk for epithelial ovarian cancer. Gynecol Oncol. 2015;139(2):253–60. doi:10.1016/j.ygyno.2015.08.024.
6. Felder M, Kapur A, Gonzalez-Bosquet J, Horibata S, Heintz J, Albrecht R, et al. MUC16 (CA125): tumor biomarker to cancer therapy, a work in progress. Mol Cancer. 2014;13:129. doi:10.1186/1476-4598-13-129.
7. Vathipadiekal V, Wang V, Wei W, Waldron L, Drapkin R, Gillette M, et al. Creation of a human secretome: a novel composite library of human secreted proteins—validation using ovarian cancer gene expression data and a virtual secretome array. Clin Cancer Res. 2015;21(21):4960–9. doi:10.1158/1078-0432.CCR-14-3173.
8. Wei SU, Li H, Zhang B. The diagnostic value of serum HE4 and CA-125 and ROMA index in ovarian cancer. Biomed Rep. 2016;5(1):41–4. doi:10.3892/br.2016.682.
9. Bowen NJ, Walker LD, Matyunina LV, Logani S, Totten KA, Benigno BB, et al. Gene expression profiling supports the hypothesis that human ovarian surface epithelia are multipotent and capable of serving as ovarian cancer initiating cells. BMC Med Genom. 2009;2:71. doi:10.1186/1755-8794-2-71.
10. Elgaaen BV, Olstad OK, Sandvik L, Odegaard E, Sauer T, Staff AC, et al. ZNF385B and VEGFA are strongly differentially expressed in serous ovarian carcinomas and correlate with

survival. PLoS One. 2012;7(9):e46317. doi:10.1371/journal.pone.0046317.
11. Mok SC, Bonome T, Vathipadiekal V, Bell A, Johnson ME, Wong KK, et al. A gene signature predictive for outcome in advanced ovarian cancer identifies a survival factor: microfibril-associated glycoprotein 2. Cancer Cell. 2009;16(6):521–32. doi:10.1016/j.ccr.2009.10.018.
12. Elgaaen BV, Olstad OK, Haug KB, Brusletto B, Sandvik L, Staff AC, et al. Global miRNA expression analysis of serous and clear cell ovarian carcinomas identifies differentially expressed miRNAs including miR-200c-3p as a prognostic marker. BMC Cancer. 2014;14:80. doi:10.1186/1471-2407-14-80.
13. Barrett T, Wilhite SE, Ledoux P, Evangelista C, Kim IF, Tomashevsky M, et al. NCBI GEO: archive for functional genomics data sets—update. Nucleic Acids Res. 2013;41(Database issue):D991–5. doi:10.1093/nar/gks1193.
14. da Huang W, Sherman BT, Lempicki RA. Systematic and integrative analysis of large gene lists using DAVID bioinformatics resources. Nat Protoc. 2009;4(1):44–57. doi:10.1038/nprot.2008.211.
15. Szklarczyk D, Franceschini A, Wyder S, Forslund K, Heller D, Huerta-Cepas J, et al. STRING v10: protein-protein interaction networks, integrated over the tree of life. Nucleic Acids Res. 2015;43(Database issue):D447–52. doi:10.1093/nar/gku1003.
16. Shannon P, Markiel A, Ozier O, Baliga NS, Wang JT, Ramage D, et al. Cytoscape: a software environment for integrated models of biomolecular interaction networks. Genom Res. 2003;13(11):2498–504. doi:10.1101/gr.1239303.
17. Bader GD, Hogue CW. An automated method for finding molecular complexes in large protein interaction networks. BMC Bioinform. 2003;4:2.
18. Xiao F, Zuo Z, Cai G, Kang S, Gao X, Li T. miRecords: an integrated resource for microRNA-target interactions. Nucleic Acids Res. 2009;37(Database issue):D105–10. doi:10.1093/nar/gkn851.
19. Gyorffy B, Lanczky A, Szallasi Z. Implementing an online tool for genome-wide validation of survival-associated biomarkers in ovarian-cancer using microarray data from 1287 patients. Endocr Relat Cancer. 2012;19(2):197–208. doi:10.1530/ERC-11-0329.
20. Wan J, Shi F, Xu Z, Zhao M. Knockdown of eIF4E suppresses cell proliferation, invasion and enhances cisplatin cytotoxicity in human ovarian cancer cells. Int J Oncol. 2015;47(6):2217–25. doi:10.3892/ijo.2015.3201.
21. Fang Y, Yu H, Liang X, Xu J, Cai X. Chk1-induced CCNB1 overexpression promotes cell proliferation and tumor growth in human colorectal cancer. Cancer Biol Ther. 2014;15(9):1268–79. doi:10.4161/cbt.29691.
22. Zhou L, Li J, Zhao YP, Cui QC, Zhou WX, Guo JC, et al. The prognostic value of Cyclin B1 in pancreatic cancer. Med Oncol. 2014;31(9):107. doi:10.1007/s12032-014-0107-4.
23. Avery-Kiejda KA, Bowden NA, Croft AJ, Scurr LL, Kairupan CF, Ashton KA, et al. P53 in human melanoma fails to regulate target genes associated with apoptosis and the cell cycle and may contribute to proliferation. BMC Cancer. 2011;11:203. doi:10.1186/1471-2407-11-203.
24. Kreis NN, Friemel A, Zimmer B, Roth S, Rieger MA, Rolle U, et al. Mitotic p21Cip1/CDKN1A is regulated by cyclin-dependent kinase 1 phosphorylation. Oncotarget. 2016. doi:10.18632/oncotarget.10330.
25. Tu Y, Kim E, Gao Y, Rankin GO, Li B, Chen YC. Theaflavin-3,3′-digallate induces apoptosis and G2 cell cycle arrest through the Akt/MDM2/p53 pathway in cisplatin-resistant ovarian cancer A2780/CP70 cells. Int J Oncol. 2016;48(6):2657–65. doi:10.3892/ijo.2016.3472.
26. Zhou J, Zhao M, Tang Y, Wang J, Wei C, Gu F, et al. The milk-derived fusion peptide, ACFP, suppresses the growth of primary human ovarian cancer cells by regulating apoptotic gene expression and signaling pathways. BMC Cancer. 2016;16:246. doi:10.1186/s12885-016-2281-6.
27. Volkov VA, Grissom PM, Arzhanik VK, Zaytsev AV, Renganathan K, McClure-Begley T, et al. Centromere protein F includes two sites that couple efficiently to depolymerizing microtubules. J Cell Biol. 2015;209(6):813–28. doi:10.1083/jcb.201408083.
28. Brendle A, Brandt A, Johansson R, Enquist K, Hallmans G, Hemminki K, et al. Single nucleotide polymorphisms in chromosomal instability genes and risk and clinical outcome of breast cancer: a Swedish prospective case–control study. Eur J Cancer. 2009;45(3):435–42. doi:10.1016/j.ejca.2008.10.001.
29. Dai Y, Liu L, Zeng T, Zhu YH, Li J, Chen L, et al. Characterization of the oncogenic function of centromere protein F in hepatocellular carcinoma. Biochem Biophys Res Commun. 2013;436(4):711–8. doi:10.1016/j.bbrc.2013.06.021.
30. Zhuo YJ, Xi M, Wan YP, Hua W, Liu YL, Wan S, et al. Enhanced expression of centromere protein F predicts clinical progression and prognosis in patients with prostate cancer. Int J Mol Med. 2015;35(4):966–72. doi:10.3892/ijmm.2015.2086.
31. Martens-de Kemp SR, Nagel R, Stigter-van Walsum M, van der Meulen IH, van Beusechem VW, Braakhuis BJ, et al. Functional genetic screens identify genes essential for tumor cell survival in head and neck and lung cancer. Clin Cancer Res. 2013;19(8):1994–2003. doi:10.1158/1078-0432.CCR-12-2539.
32. Venere M, Horbinski C, Crish JF, Jin X, Vasanji A, Major J, et al. The mitotic kinesin KIF11 is a driver of invasion, proliferation, and self-renewal in glioblastoma. Sci Transl Med. 2015;7(304):304ra143. doi:10.1126/scitranslmed.aac6762.
33. Mirzaa GM, Enyedi L, Parsons G, Collins S, Medne L, Adams C, et al. Congenital microcephaly and chorioretinopathy due to de novo heterozygous KIF11 mutations: five novel mutations and review of the literature. Am J Med Genetics Part A. 2014;164A(11):2879–86. doi:10.1002/ajmg.a.36707.
34. Seo DW, You SY, Chung WJ, Cho DH, Kim JS, Oh JS. Zwint-1 is required for spindle assembly checkpoint function and kinetochore-microtubule attachment during oocyte meiosis. Sci Rep. 2015;5:15431. doi:10.1038/srep15431.
35. Endo H, Ikeda K, Urano T, Horie-Inoue K, Inoue S. Terf/TRIM17 stimulates degradation of kinetochore protein ZWINT and regulates cell proliferation. J Biochem. 2012;151(2):139–44. doi:10.1093/jb/mvr128.
36. Hammond SM. An overview of microRNAs. Adv Drug Deliv Rev. 2015;87:3–14. doi:10.1016/j.addr.2015.05.001.
37. Zuberi M, Mir R, Das J, Ahmad I, Javid J, Yadav P, et al. Erratum to: Expression of serum miR-200a, miR-200b and miR-200c as candidate biomarkers in epithelial ovarian cancer and their association with clinicopathological features. Clin Transl Oncol. 2015;17(10):840. doi:10.1007/s12094-015-1355-2.
38. Meng X, Muller V, Milde-Langosch K, Trillsch F, Pantel K, Schwarzenbach H. Diagnostic and prognostic relevance of circulating exosomal miR-373, miR-200a, miR-200b and miR-200c in patients with epithelial ovarian cancer. Oncotarget. 2016;7(13):16923–35. doi:10.18632/oncotarget.7850.
39. Xu S, Tao Z, Hai B, Liang H, Shi Y, Wang T, et al. miR-424(322) reverses chemoresistance via T-cell immune response activation by blocking the PD-L1 immune checkpoint. Nat Commun. 2016;7:11406. doi:10.1038/ncomms11406.
40. Xia B, Li H, Yang S, Liu T, Lou G. MiR-381 inhibits epithelial ovarian cancer malignancy via YY1 suppression. Tumour Biol. 2016. doi:10.1007/s13277-016-4805-8.